2021 IEEE 17th International Conference on Automation Science and Engineering (CASE)
August 23-27, 2021. Lyon, France

Task Allocation in Multi-Robot Systems Based on the Suitability Level of the Individual Agents

Omar Al-Buraiki, *Member IEEE*, and Pierre Payeur, *Member IEEE*

2021 IEEE 17th International Conference on Automation Science and Engineering (CASE) | 978-1-6654-1873-7/21/$31.00 ©2021 IEEE | DOI: 10.1109/CASE49439.2021.9551466

***Abstract*— This paper examines task allocation in multi-robot systems in the context where a suitability level of the specialized robots is considered. Based on the assumption that each individual agent possesses specialized functional capabilities and that the expected tasks impose specific requirements, a formulation of the agents' specialization is defined to estimate individual agents' task allocation probabilities. The original task allocation process involves a centralized matching scheme to associate each agent's suitability level with corresponding detected tasks. Then, the task-agent matching scheme is expanded to coordinate the most specialized agent or group of agents while also considering availability factors. Early experimental results are presented and analyzed to demonstrate the effectiveness of the proposed framework.**

I. Introduction

The goal of this research is to evolve the coordination of a heterogeneous group of robots to be well functioning as a cooperative team, under consideration of the respective agents' specialization. The resulting team should be able to optimize the overall level of competence that the robots can offer while being assigned to a series of tasks, where each task is to be mastered by the proper individual agent or by many qualified agents collaborating together. The focus in this paper is on developing and exploiting an analog formulation of the individual robots' specializations to best satisfy the specific requirements imposed by given tasks.

II. Related Work

A sequence of task-agent allocations to minimize the task duration or energy consumption for a team of heterogeneous mobile robots is introduced in [1]. The stick-pulling problem [2] is considered in [3] to investigate the advantages of specializing robotic agents in the case where two mobile robots execute a cooperative task. A task partitioning strategy is also introduced in [4]. Given that behavioral-based specialization [5] in a multi-robot system can emerge as the result of interactions among the robots and with the environment, a task-agent assignment probabilistic algorithm is introduced in [6] to partition the environment to a grid of cells. The available robots in each cell are assigned to the targets located with the same cell. Alternatively, a probabilistic model to define object-action relevance is developed in [7]. A probabilistic threshold is proposed in [8] to control robots that perform a food foraging process and that need to leave the nest to search for food.

To increase the efficacy of the task allocation process introduced in [9] and to take advantage of task-oriented suitability levels for robots possessing specialized functionalities, a non-binary formulation of the robotic agents' competence levels is proposed in this paper to support a probabilistic task-agent matching process. It leads to an efficient strategic allocation of the individual specialized robotic agents to specific corresponding tasks as a form of collaboration in a multi-robot system.

III. Proposed Framework

The proposed approach forms a probabilistic specialty-based task allocation mechanism for different robots that are equipped with specialized capabilities to best match with constrained tasks detected in their environment. The proposed solution considers the team members to be different at their functionality level (e.g. on-board actuators or sensors, communication and reasoning capabilities). A schematic diagram of the proposed framework is shown in Fig. 1. The control space tackles the robots' dynamics control and navigation, whose design aspects are detailed in our previous work [10]. The specialization space, addressed in this paper, pays close attention to the match between the task requirements and the individual robots' specialized capabilities, encoded as an agent-specific suitability level.

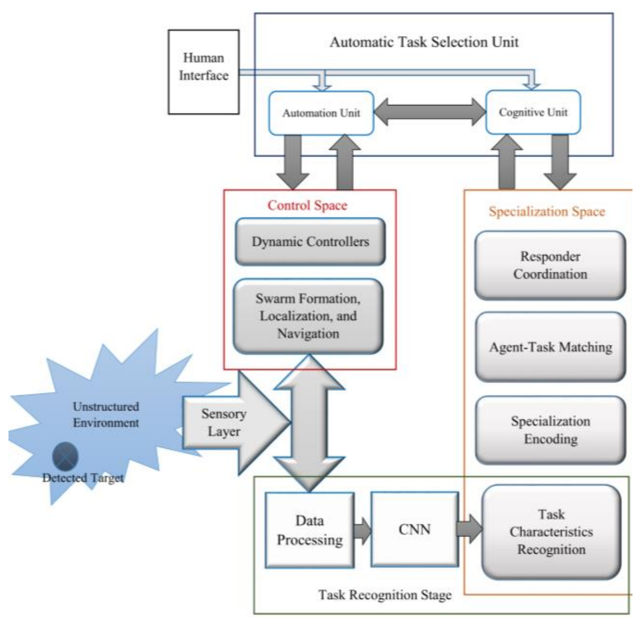

Fig. 1 Proposed architecture for specialized agents task allocation.

In the specialization space, a probabilistic approach is developed to match visual features perceived on detected tasks with robot specialties. It relies on an uncertain representation of the observed features [11] on target objects contained in the robotic swarm environment. The framework designed in this paper aims strictly at the coordination of the suitable responders to the corresponding tasks. An “automatic task selection unit” (ATSU), shown in Fig. 1, is responsible for the decision-making process and is detailed in [12].

IV. Task Characteristics Recognition

The dominant features on the considered target objects are separated into classes. The group of features $\boldsymbol{X}_k$ on a class C_l that can be observed on each target type are encoded as a vector of F sample features, that is $\boldsymbol{X}_k = \{x_j : j = 1, \cdots, F\}$, where $x_j \in \mathcal{R}^2$ is a Gaussian distributed random sample of a two-dimensional spatial feature that is observed with mean μ and variance σ^2. Also, $k = 1,2, \ldots, T$, where T is the maximum number of different target object classes that can be detected in the robots' workspace, $\boldsymbol{X} = [\, \boldsymbol{X}_k : k = 1,2, \ldots, T]$. An assumption is also made that every group of features, $\boldsymbol{X}_k$, is associated with one specific class, $C_l : l = 1,2, \ldots, T$. To ensure the mapping between appropriate agents and corresponding tasks, each class is associated with an action of a given nature to be performed by a specialized capability of a given robot. The task space, $\boldsymbol{X}$, is therefore comprised of $F \times T$ features that characterize T possible target objects that are associated with the specialized capabilities available among the members of the robotic team. The probability of the observed features, $\boldsymbol{X}_k$, that characterize each class C_l, is estimated by the Bayesian rule:

$$P(C_l|\boldsymbol{X}_k) = \frac{p(\boldsymbol{X}_k|C_l)P(C_l)}{p(\boldsymbol{X}_k)} \tag{1}$$

where $p(\boldsymbol{X}_k|C_l)$ is the class-conditioned probability density function that describes the Gaussian distribution of the group of features, $\boldsymbol{X}_k$, in each predefined target object class, C_l; $P(C_l)$ is a prior probability of the class C_l, which is evaluated from the given training dataset. $p(\boldsymbol{X}_k)$ is the probability density function of $\boldsymbol{X}_k$ over the entire dataset considered. Since all quantities in Eq. (1) are a function of C_l, the denominator in Eq. (1) can be considered a normalization constant, substituted by $\frac{1}{\xi}$, to ensure that the left-hand side integrates to one [11]. Thus:

$$P(C_l|\boldsymbol{X}_k) = \xi\, p(\boldsymbol{X}_k|C_l)P(C_l) \tag{2}$$

The detected feature, $x_j \in \boldsymbol{X}_k$, on a target is associated to the class that has the maximum posterior probability $P(C_l|\boldsymbol{X}_k)$.

V. Suitability-based Task-Agent Matching

For a given matching assignment, an agent responds to specific task requirements when the agent's specialty offers a sufficient suitability. However, a given agent can be suitable for different tasks with different competence levels according to how a robot is built or equipped. The proposed approach evaluates the respective agents' suitability to be assigned to the task and selects the most qualified agent or group of agents, depending on the nature of the actions to be performed.

A. Analog Specialization Encoding

A team of robots $\{R_i, i = 1,2, \ldots, a\}$ consists of a robots, R_i, and provides T different specialized action capabilities. To represent a given agent's specialty in an abstract way, an agent's specialty vector, $\boldsymbol{S}_i : \{\mathrm{s}_k, k = 1,2, \ldots, T\}$ where $\boldsymbol{S}_i \in \mathcal{R}^{1\times T}$, introduced in [9], is encoded with a set of analog values. Mimicking the development of human competence through training or experience, it is proposed to encode each agent's entries of $\boldsymbol{S}_i \in \mathcal{R}^{1\times T}$, over the continuous range of 0 to 1, such that $\mathrm{s}_k \in [0 \;\; 1]$. Each entry represents the relative level of an agent's specialized capabilities, from low qualification (0) to the most specialized capability (1):

$$\mathrm{s}_k = \begin{cases} 0 < \mathrm{s}_k \leq 1 & : R_i \text{ has a given qualification level } \mathrm{s}_k \\ 0 & : R_i \text{ is not qualified} \end{cases} \tag{3}$$

$0 < \mathrm{s}_k \leq 1$ means that the robot possesses a corresponding level of a specialized capability to tackle a task of a class C_l, recognized from the observed group of features, $\boldsymbol{X}_k$.

B. Task-Agent Matching with Suitability Level

The confidence level of each robot to properly perform a task associated with a detected target object is defined as:

$$\hat{\varphi}_{R_i} = \boldsymbol{S}_i \widehat{\boldsymbol{P}}_T \tag{4}$$

$\hat{\varphi}_{R_i} \in \mathcal{R}^{1\times 1}$ is the specialty fitting confidence level achieved by an agent R_i of identity, i, based on the constraints raised by the detected classes of a given target object. $\widehat{\boldsymbol{P}}_T \in \mathcal{R}^{T\times 1}$ represents the probability transition vector of the detected classes, formulated as uncertain measurements from target objects recognition. This is a function of the estimated posterior probabilities, Eq. (2), defined as:

$$\widehat{\boldsymbol{P}}_T = \left[\sum_{k=1}^{T} P(C_1|\boldsymbol{X}_k) \;\; \sum_{k=1}^{T} P(C_2|\boldsymbol{X}_k) \;\; \cdots \;\; \sum_{k=1}^{T} P(C_T|\boldsymbol{X}_k) \right]^T \tag{5}$$

To formulate the task-agent specialty matching in a probabilistic form, the concepts of probability theory are adopted [13]. The main concepts of the probabilistic model are: 1) An *agent's sample space:* the sample space is represented by the encoded specialties of each robotic agent, indicated by the vector, $\boldsymbol{S}_i$. The possible sample space of R_i is modelled as $\varphi_{R_i} \in \mathcal{R}^{1\times 1}$, defined in Eq. (8). 2) An *events space*: this is introduced as an estimated fitting confidence level, $\hat{\varphi}_{R_i}$, which is a function of the agent's specialization vector $\boldsymbol{S}_i$ and uncertain measurements from target object detections, $\widehat{\boldsymbol{P}}_T$, introduced in Eq. (5). 3) A *probability function* associates with each event in the agent's *events space* a probability as a real number in the range [0, 1]. This forms the respective agents' specialty matching probability, which is defined as follows:

$$Q_i = \frac{\hat{\varphi}_{R_i}}{\varphi_{R_i}} \tag{6}$$

The specialty matching matrix, $\boldsymbol{Q} \in \mathcal{R}^{a\times a}$, can be formed as:

$$\boldsymbol{Q} = diag\left[\frac{\hat{\varphi}_{R_1}}{\varphi_{R_1}}, \frac{\hat{\varphi}_{R_2}}{\varphi_{R_2}}, \cdots, \frac{\hat{\varphi}_{R_{a-1}}}{\varphi_{R_{a-1}}}, \frac{\hat{\varphi}_{R_a}}{\varphi_{R_a}} \right] \tag{7}$$

where φ_{R_i} is the sum of the encoded basis of the agent's specialized capabilities defined in its specialization vector $\boldsymbol{S}_i$, defined as:

$$\varphi_{R_i} = \sum_{k=1}^{T} \mathrm{s}_k \tag{8}$$

It is also worth noting that the sum of specialized capability levels associated with a given agent, $\sum_{k=1}^{T} \mathrm{s}_k$, is not constrained to unity. This provides additional flexibility in the selection of the agents involved in the swarm.

C. Qualified Responders' Coordination

It is important to support realistic scenarios in which a robot may not always be available because of a dead battery or because it was already allocated to another task. To tackle such circumstances, the proposed framework integrates an agents' availability state, $\boldsymbol{\vartheta}_{Av}$, beyond the specialty representation, $\boldsymbol{Q}$. The agents' availability, $\boldsymbol{\vartheta}_{Av}$, is meant to ensure the replacement of unavailable robotic agents with available ones. The availability vector, $\boldsymbol{\vartheta}_{Av} \in \mathcal{R}^{a\times 1}$, is defined based on the current internal status of each robot. At the time of robotic swarm deployment, the internal flag of the deployed agents is raised to "available" while the internal flag of agents that are not available is set to "withdrawn". When active, the availability flag keeps the agent's task allocation probability operational and detected tasks are assigned to an available agent when its estimated fitting confidence level, $\hat{\varphi}_{R_i}$, is optimal. In contrast, agents with an internal flag set to "withdrawn" are deactivated, and the task allocator searches for an alternative "available" agent to accomplish the mission set by a detected task. When an available agent is assigned to a given task, then its availability state is changed to "busy" until the task is fulfilled. The availability vector, $\boldsymbol{\vartheta}_{Av} \in \mathcal{R}^{a\times 1}$, is defined as:

$$\vartheta_{Av_i} = \begin{cases} 1, & R_i \; is \; "available" \\ 0, & R_i \; is \; "withdrawn" \; or \; "busy" \end{cases} \tag{9}$$

The coordination scheme operates from the cumulation of two components: 1) the specialty matching probabilities, $\boldsymbol{Q}$; and 2) the availability state, $\boldsymbol{\vartheta}_{Av}$, of each robotic agent. Therefore, the suitability-based matching scheme is overall defined as:

$$\boldsymbol{\Psi} = \boldsymbol{Q}\, \boldsymbol{\vartheta}_{Av} \tag{10}$$

$\boldsymbol{\Psi} \in \mathcal{R}^{a\times 1}$ returns task allocation probabilities with respect to the detected task for the available agents, or 0 for withdrawn or busy units.

To vary the dynamic response according to operational conditions, a human supervisor should remain involved as a supervisor in the task allocation process and given a role to initialize or control a task allocation response threshold but should not need to intervene frequently. For this purpose, a minimum fitting threshold (MFT), η, is implemented as a safety measure that guarantees a minimum qualification or suitability level below which no agent will respond. The human operator sets the MFT value for the system, either before the deployment of the robots or during the operation. This way, human skills can be shared with the robots by varying this parameter dynamically, and the minimum required level of trust (MFT) in the recognized target object can influence the coordination before robots are put in action. Given that one of the overall objectives of this approach is to reduce the cognitive load on the operator, pre-setting the distribution of MFT over predefined ranges showed that it can reduce the number of times the human operator needs to intervene on the MFT setpoint and simplify the operation. Therefore, the desired MFT, η, is overall defined as $\eta \in (0\ 1]$, but is distributed over two predefined ranges representing respectively a low specialty fitting level (LSFL), suitable for less critical tasks, and a high specialty fitting level (HSFL), for when highly specialized intervention is required:

$$\begin{cases} LSFL: & 1 < \eta \leq \tau, \\ HSFL: & \tau < \eta \leq 1, \end{cases} \tag{11}$$

This formulation ensures that only a satisfactory suitability level, above the set MFT, estimated as a specialty matching probability, $\boldsymbol{Q}$, can initiate the task allocation process. Therefore, $\boldsymbol{\Psi}$, defined in Eq. (10), is further refined to only consider the task allocation suitability levels of the available agents that achieve the desired MFT, and is reformulated as:

$$\boldsymbol{\Psi}_{MFT} = [\Psi_{MFT_1}, \Psi_{MFT_2}, \cdots, \Psi_{MFT_a}]^T \tag{12}$$

and

$$\Psi_{MFT_i} = \begin{cases} \Psi_i, & \mid \Psi_i \geq \eta : \Psi_i \in \boldsymbol{\Psi} \\ 0, & \mid \Psi_i < \eta : \Psi_i \in \boldsymbol{\Psi} \end{cases} \tag{13}$$

Accordingly, the qualified and available agents are automatically selected and allocated to the detected tasks considering the human supervisor's strategic guidance, triggered by parameter τ. The identification index of the best-suited available agent above the MFT is given by:

$$\emptyset_{BEST\ RESPONDER\ INDEX} = i \mid i \in max\,\{\boldsymbol{\Psi}_{MFT}\} \tag{14}$$

The max operator is used to extract the identification of the agent with the highest suitability level.

VI. Experimental Validation in Simulation

The proposed approach is experimentally validated by considering a set of $T = 5$ classes of target objects to be potentially detected in an environment that surrounds a multi-robot system consisting of $a = 8$ specialized robotic agents, that can intervene each with their predefined qualification levels when facing a given type of task. Table 1 defines the analog encoding preset for the 8 agents based on their respective suitability level to each task. These levels are estimated, often at time of construction or configuration of a robotic agent, according to its mechanical, electronic, or computational capabilities. For example, considering that agent R_1 is a ground vehicle equipped to provide basic first-aid care services (task type T_{F_1}), the suitability level of this robot for this type of task can arbitrarily be set to 0.6 in the agents' analog specialization encoding, defined in section V.A and represented in its specialty vector, $\boldsymbol{S}_1$, detailed in Table 1.

TABLE 1: Analog encoding of specialized functionalities for a group of 8 robotic agents to meet the requirements of 5 different task types.

Agents' analog specialty vectors	Task types (First-aid care with increasing complexity (T_{F_1} to T_{F_5}))				
	T_{F_1}	T_{F_2}	T_{F_3}	T_{F_4}	T_{F_5}
$\boldsymbol{S}_1$	0.6	0.2	0	0	0
$\boldsymbol{S}_2$	0.2	0.7	0	0	0
$\boldsymbol{S}_3$	0.5	0	0.5	0	0
$\boldsymbol{S}_4$	0.4	0.3	0.4	0	0
$\boldsymbol{S}_5$	0	0.4	0.6	0	0
$\boldsymbol{S}_6$	0	0	0.4	0.8	0
$\boldsymbol{S}_7$	0	0	0	0.55	0.45
$\boldsymbol{S}_8$	0	0	0	0.5	0.5

Considering that the same agent is less adapted to provide more advanced levels in emergency care (e.g. task type T_{F_2}), this fact can be encoded with a lower functionality level at 0.2, also displayed in Table 1. For demonstration purpose, the following test cases consider that a low specialty fitting level ($LSFL$) is sufficient for an agent to be assigned a detected task through the proposed task-agent matching process detailed in section V and with an imposed MFT value of $\eta = 0.3$.

A. General Framework Validation

This test case initially considers that all team members defined in Table 1 are available for the task assignment process whenever a compatible task is detected in the environment of the robotic swarm. Fig. 2 depicts the situation where a target object of type T_{F_1} (e.g. a minor car accident) is detected with a confidence of 80% by a unmanned aerial vehicle (UAV) (shown in red) conducting surveillance over an area. The UAV collects data from the workspace and feeds the target detection stage. The task allocation process results in different suitability levels with the detected task, considering Eq. (12). The numerical results are detailed in Table 2.

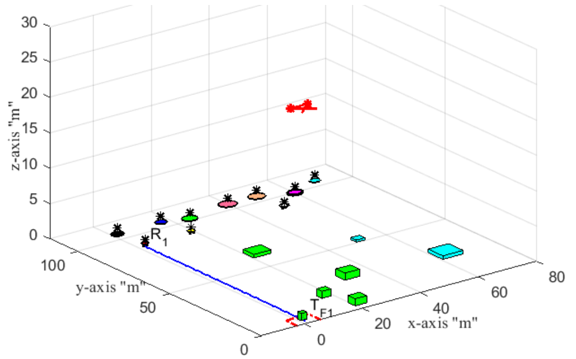

Fig. 2 Robot R_1 offering highest suitability level to target type T_{F_1}.

TABLE 2: SUITABILITY-BASED TASK ALLOCATION WITH RESPECT TO A TASK T_{F_1}.

$\hat{P}_T$	ID#	$(\boldsymbol{Q})$	$(\boldsymbol{\vartheta}_{Av})$ 1:Available 0:Withdrawn or Busy	Suitability level $\boldsymbol{\Psi}_{MFT}$	MFT (η)
T_{F_1} 0.8	R_1	0.6	1	**0.6***	
	R_2	0.18	1	---	
	R_3	0.4	1	0.4	0.3
	R_4	0.3	1	0.3	

*selected agent assigned to detected task.

The agent R_1 is the most qualified agent for this situation with suitability level of 0.6, which is obtained with Eq. (4) from the combination of the confidence in the detected task (0.8) and the agent's specialty level (0.6) from Table 1, and normalized on the basis of all agent R_1's qualifications as per Eq. (6). That is, $Q_1 = (0.8*0.6)/(0.6+0.2) = 0.6$. Given that all agents are considered available ($\vartheta_{Av_i} = 1, \text{for } i \in [1\ 4]$) in this test case, the probabilistic qualification level, Q_1, carries directly through Eq. (10) and into Eq. (12). Similarly, agents R_3 and R_4 present the second and third highest suitability levels at 0.4 and 0.3, respectively. The suitability of all three agents satisfies the set MFT at 0.3, Eq. (13).

On the other hand following the same computational process, agent R_2 offers a suitability level to task of type T_{F_1} of only 0.18, which is lower than the minimum level (MFT) that the system requires for the task allocation to proceed on an agent. As a result, agent R_2 cannot be allocated to the task (T_{F_1}) and is discarded. Therefore, as per Eq. (14), the task allocator selects the most suitable agent as a first specialized responder to the detected target, and the system automatically assigns R_1.

B. Validation with Management of Agents' Availability

Whenever an agent is assigned to a given task, as in section VI.A, or must be removed from the list of available responders due to a failure, the corresponding agent's availability flag is changed to "busy" or "withdrawn", as per Eq. (9). In such circumstances, the proposed task allocator exhibits the necessary flexibility to still rank and determine the most qualified agents by automatically substituting the unavailable agents with alternative qualified agents. Formally considering the proposed availability states, $\boldsymbol{\vartheta}_{Av}$ in Eq. (9), as part of the suitability level estimation in Eq. (10) is an original feature of the proposed framework which significantly increases its functionality and reliability. In this second case, the task allocator, Eq. (12), computes the suitability level for all "available" agents to respond to a target detected with a confidence level of 75%. Fig. 3a illustrates a target object of type T_{F_2} detected over the workspace while initially considering that all agents are available, Table 3A (4th column from the left). As shown, the agents offer task allocation suitability levels with respect to T_{F_2} ranging from 0.19 to 0.58, computed in the same way as detailed in section VI.A. Agent R_2 has the highest suitability level with 0.58, and agent R_5 offers the second-highest suitability level (0.3) that just satisfies the minimum requirement (MFT) set through strategic guidance by a human operator. However, agent R_1 and R_4 exhibit lower suitability levels to 0.19, and 0.2 respectively, which leads to discard these agents from the task allocation process. As a result, the framework ranks the estimated suitability levels in descending order and selects the most qualified one, Eq. (14), that is agent R_2 to respond to the detected task T_{F_2}.

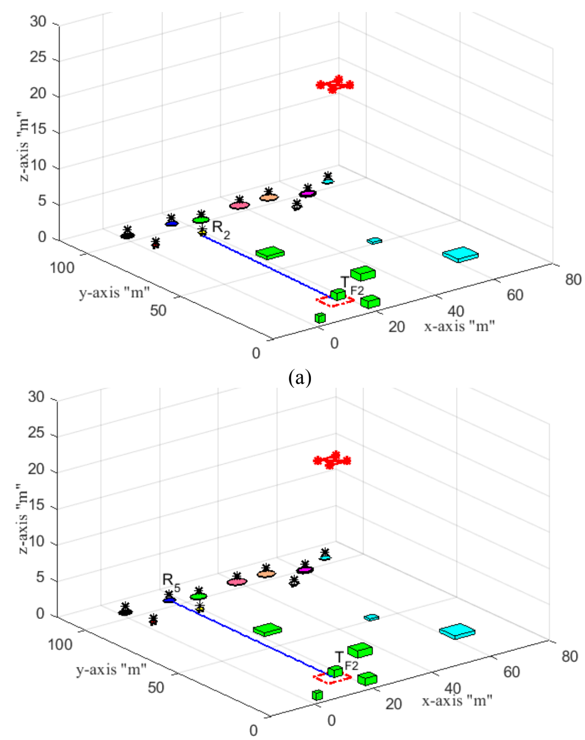

(a)

(b)

Fig. 3 Successive allocation of robotic agents in decreasing order of suitability to perform a detected target of type T_{F_2}, with consideration of availability status for the agents.

TABLE 3: TASK ALLOCATION WITH SUITABILITY LEVELS, WHEN:
A) THE MOST SUITABLE AGENTS ARE "AVAILABLE".

$\hat{P}_T$	ID#	$(\boldsymbol{Q})$	$(\boldsymbol{\vartheta}_{Av})$ *1:Available 0:Withdrawn or Busy*	*Suitability level* $\boldsymbol{\Psi}_{MFT}$	*MFT (η)*
T_{F_2} 0.75	R_1	0.19	**1**	---	0.3
	R_2	0.58	**1**	**0.58***	
	R_4	0.2	**1**	---	
	R_5	0.3	**1**	0.3	
B) THE MOST SUITABLE AGENTS ARE "BUSY" OR "WITHDRAWN"					
T_{FE_2} 0.75	R_1	0.19	**1**	---	0.3
	R_2	0.58	**0**	---	
	R_4	0.2	**1**	---	
	R_5	0.3	**1**	**0.3***	

Subsequently, if further support is required to perform the task on target type T_{F_2} once R_2 reaches the "busy" state, as indicated in Table 3B (4th column from the left), the system runs iteratively and assigns the next most suitable and still available agent, R_5, as depicted in Fig. 3b. The respective suitability levels for the agents remain unchanged, however the availability factor, $\boldsymbol{\vartheta}_{Av}$, in Eq. (10) influences the outcomes of the task allocation process as detailed in Table 3B. This case demonstrates that formally considering the agents' availability provides significant advantages. As such, when the most specialized agent is "busy" or "withdrawn", the system responds reliably and successively assigns the next most suitable agent with respect to the specialized functionalities required to handle the detected task.

VII. VALIDATION WITH REAL ROBOTS

Given that task allocation and robots coordination strategies find a growing number of applications in the real world, the proposed task allocation framework was implemented in a centralized decision stage remotely controlling the operation of a small group of physical mobile robots. The latter involved two commercially available platforms: one TurtleBot3 Waffle Pi and one TurtleBot3 Burger [15]. A color camera separately integrated in the environment serves to detect landmark target objects uniquely identified by a combination of two-color stripes that provide different visual signatures: red-green, and blue-red respectively. For the sake of simplicity in validating the proposed approach, each color combination represents a task type to be performed and is associated, based on the robots' embedded functionalities, with one of the agents considered. The related qualifications are marked by a corresponding color-coded landmark mounted over each of the mobile robots, as shown in Fig. 5. The robotic agents' qualifications are represented with the proposed analog encoding which assigns each agent different levels of competence, in the range [0 1], as per Eq. (3). The experimental decision layer uses a central processing unit (CPU) on a laptop running the Linux (Ubuntu) operation system built upon a ROS navigation stack. The latter ensures communication between the central unit and the two robots via a Wi-Fi network. Communications, robots' localization, and path-planning capabilities are mastered by ROS.

In experiments with physical robots, a See3CAM_130 USB color camera [16] is used to detect the dual-color features on each landmark task object. The recognition stage exploits the detection of a pair of colors in the Hue-Saturation-Value (HSV) color space representation, depicted in Fig. 4 for hue values over the range [0 179].

Fig. 4 Hue-Saturation-Value color space.

A tolerance on the hue value of ± 5 around the predicted hue is applied to deal with imperfection in the imaging process and variability of perception due to the environment. To convert this variability on the color detection results provided by the camera into a confidence level on the detection of a target object corresponding to a task of a given type, the following formula is derived:

$$P_{C_l} = \frac{10 - [actual\ hue - |detected\ hue|]}{10} \tag{15}$$

In order to support integration with the task allocation stage, the output of the object detection stage, Eq. (5), is defined as follows:

$$\hat{\boldsymbol{P}}_T = \left[P_{C_1}, P_{C_2}\right]^T \tag{16}$$

where $C_l: l = 1:2$ denote the two combinations, or classes, of color features considered in this test case, respectively that is red-green and blue-red. $P_{C1} \sim P_{C2}$ correspond to the recognition confidence level on a target object features associated with each class of task.

In the considered test case, shown in Fig. 5, the multi-agent system consists of the two available agents: a Waffle (associated with the blue-red task) and a Burger (associated with the red-green task) Turtlebot3 robots. Accordingly, the specialization vectors, $\boldsymbol{S}_i$, of the robots are defined in Table 4.

TABLE 4: ANALOG SPECIALIZATION ENCODING FOR A PAIR OF PHYSICAL ROBOTS

Agent Name	*Specialty vector*	*Red feature*	*Blue feature*	*Green feature*
Burger	$\boldsymbol{S_1}$	0.5	0	0.5
Waffle	$\boldsymbol{S_2}$	0.5	0.5	0

An experimental trial is represented in Fig. 5 at different stages of the allocation process, and numerical values are detailed in Table 5 where the confidence on recognizing the red color on the target object is estimated as 70%, while the blue color is detected with confidence equal to 90%. No green color (0%) is perceived on the target object. Considering also that both robotic agents are initially available, $\boldsymbol{\vartheta}_{Av} = 1$, the respective specialty matching probability for each robot is computed, Eq. (6). Considering a minimum fitting threshold (MFT) set at 0.3, the most suitable agent is identified with Eq. (14). Given that the Waffle agent is more qualified to tackle a blue-red task type, it is selected and directed toward the target object, while the Burger agent remains in proximity in case a second round of allocation is needed to complete the task.

Results from experiments with real robots showed that the proposed approach can realistically be applied in practice while considering visual perception on target objects to condition how specialized robotic agents are allocated to corresponding tasks that impose specific constraints.

TABLE 5: AVAILABLE AGENTS' MATCHING PROBABILITIES AND SUITABILITY LEVELS WITH RESPECT TO A TARGET WITH BLUE AND RED COLORS

Target color features recognition confidence level	*Agent name*	*Target-agent specialty matching probability* ($\boldsymbol{Q}$)	*Agents' Availability 1:Available 0:Withdrawn* ($\boldsymbol{\vartheta}_{Av}$)	*Available qualified agents' suitability level* ($\boldsymbol{\Psi}_{MFT}$)	*MFT* (η)
Red: 0.70	Burger	0.35	**1**	0.35	
Blue: 0.90	Waffle Pi	0.80	**1**	**0.80***	0.3
Green: 0.00					

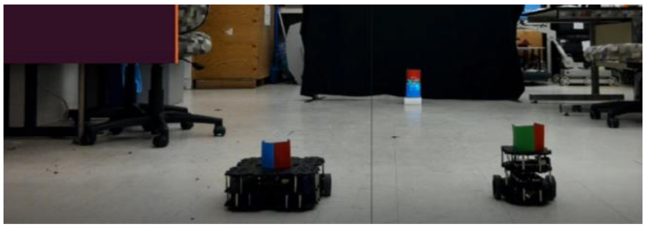

(a) t = 5 sec.: Searching for a target.

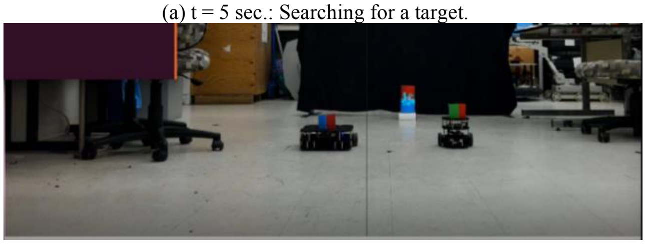

(b) t = 18 sec.: Selection of the most qualified robot.

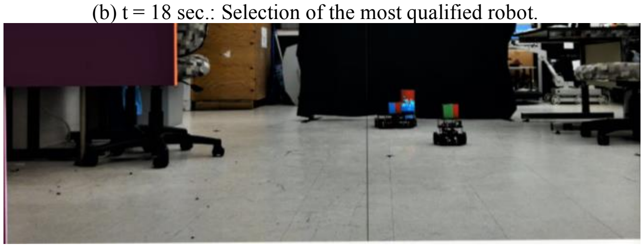

(c) t = 30 sec.: Most qualified robot completing the task.

Fig. 5 Task allocation sequence on a pair of robotic agents specialized to perform color-coded tasks.

VIII. CONCLUSION

This paper introduces a task allocation framework that relies on an analog encoding of specialized functionalities embedded on individual robotic agents that operate as a swarm. An original solution to the task allocation process emerges for heterogeneous groups of agents where every individual possesses precise mechanical, sensing, or computational characteristics to best process tasks that impose specific requirements. The flexibility of the task allocation process is increased by formally taking into consideration the agents' availability state along with their specialty-based suitability level when facing specific tasks. The latter are detected from visual sensors and characterized by confidence levels on target objects detection as made possible with modern deep learning object detection approaches. As such, the proposed framework evolves task allocation processing beyond classical methods that often aim to optimize response time and energy management or consider essentially uniform and identical entities in the definition of a robotic swarm. Experimental results in simulation and with physical robots demonstrate that the expected behavior is achieved in the coordination of a variable number of robotic agents with specialized functionalities.

ACKNOWLEDGEMENTS

The authors wish to acknowledge support from the Hadramout Foundation toward the graduate studies of the first author and appreciate Paulo Cardoso's assistance during the experimental validation on physical robots.

REFERENCES

[1] Sadeghi, A., and Smith, S. L. "Heterogeneous Task Allocation and Sequencing via Decentralized Large Neighborhood Search." *Unmanned Systems*, vol. 5, no. 02, pp. 79-95, 2017.

[2] Ijspeert, A., Martinoli, A., Billard, A., and Gambardella, L. M. "Collaboration through the Exploitation of Local Interactions in Autonomous Collective Robotics: The Stick Pulling Experiment." *Autonomous Robots*, vol. 11, no. 2, pp. 149–171, 2001.

[3] Hsieh, M. A., Halász, Á., Cubuk, E. D., Schoenholz, S., and Martinoli, A. "Specialization as an optimal strategy under varying external conditions." *IEEE International Conference in Robotics and Automation,* vol. 12, pp. 1941-1946, May 2009.

[4] Buchanan, E., Pomfret, A., and Timmis, J. "Dynamic Task Partitioning for Foraging Robot Swarms." *International Conference on Swarm Intelligence*, pp. 113-124, Springer International Publishing, 2016.

[5] Trueba, P., Prieto, A., Bellas, F., and Caamaño P. "Specialization analysis of embodied evolution for robotic collective tasks." *Robotics and Autonomous System,* vol. 61(7), pp. 682-693, July 2013.

[6] Smith, S. L., and Bullo, F. "Target assignment for robotic networks: Worst-case and stochastic performance in dense environments." *IEEE Conference in Decision and Control*, pp. 3585-3590, 2007.

[7] Lang, T., and Toussaint, M. "Relevance grounding for planning in relational domains." *Joint European Conference on Machine Learning and Knowledge Discovery in Databases*, pp. 736-751, Springer, Berlin, Heidelberg, Sep. 2009.

[8] Yasuda, T., Kage, K., and Ohkura, K. "Response threshold-based task allocation in a reinforcement learning robotic swarm." *IEEE International Workshop in Computational Intelligence and Applications,* pp. 189-194, 2014.

[9] Al-Buraiki, O., Wu, W., and Payeur, P., "Probabilistic Allocation of Specialized Robots on Targets Detected Using Deep Learning Networks." *Robotics,* 9(3), 54, July 2020.

[10] Al-Buraiki, O., Payeur, P., and Castillo, Y. R. "Task switching for specialized mobile robots working in cooperative formation." *Proc. of the IEEE International Symposium in Robotics and Intelligent Sensors*, pp. 207-212, Tokyo, Japan, Dec. 2016.

[11] Bishop, C. M. "Pattern Recognition and Machine Learning." *Springer*, New York, 2016.

[12] Al-Buraiki, O., Payeur, P., and Busquia, H. M. "Automatic Task Selection from Targets Recognition for Swarm Mobile Robots with Specialized Agents." MDPI *Proceedings*. vol. 2 (3)-116, 2017.

[13] Papoulis, A., and Pillai, S. U. "Probability, random variables, and stochastic processes." *Tata McGraw-Hill Education*, New York, 2002.

[14] Al-Buraiki, O., and Payeur, P. "Task-Agent Assignation Based on Target Characteristics for a Swarm of Specialized Agents." *Annual IEEE International Systems Conference*, pp. 268-275, Orlando, April 2019.

[15] "Overview" ROBOTIS e-Manual. 2020. [Online]. Available: http://emanual.robotis.com/docs/en/platform/turtlebot3/overview/ [Accessed: July 25, 2020].

[16] "See3CAM_130- Documents," e-con Systems, 2020. [Online]. Available: https://www.e-consystems.com/doc_13MP_autofocus_USB3_Camera.asp [Accessed: July 25, 2020].